ARTICLE

Synthesis of small water-soluble diazirine-functionalized gold nanoparticles and their photochemical modification

Sara Ghiassian, Mark C. Biesinger, and Mark S. Workentin

Abstract: Dual water and organic solvent soluble 3-aryl-3-(trifluormethyl) diazirine-functionalized gold nanoparticles (AuNPs) were prepared through a place exchange reaction from triethylene glycol monomethyl ether (EG$_3$-Me) capped AuNPs. These nanoparticles were fully characterized using ^{1}H and ^{19}F nuclear magnetic resonance (NMR) spectroscopy, transmission electron microscopy (TEM), thermogravimetric analysis (TGA), and X-ray photoelectron spectroscopy (XPS). TGA along with ^{1}H NMR data allowed the determination of 15% incorporation of diazirine (Diaz) ligands onto mixed monolayer AuNPs, while TEM images showed an average diameter of 2.3 ± 0.5 nm. This information led to the estimated molecular formula of Au$_{400}$ (S-EG$_4$-Diaz)$_{40}$ (S-EG$_3$-Me)$_{230}$ for these AuNPs. It is noteworthy that high-resolution XPS was a powerful tool for quantitative analysis. Irradiation of the diazirine capped AuNPs resulted in nitrogen extrusion and the formation of a highly reactive carbene with evidence of a portion of the reaction proceeding via the diazo intermediate and thus requiring a second photon for activation. The carbene species generated was utilized to tether the attached AuNPs via insertion into C=C or O–H functionality inherent on various substrates. Here, we demonstrated that photolysis of the diazirine modified AuNPs in the presence of a variety of model carbene scavengers led to clean and efficient insertion products while maintaining their solubility in polar solvents.

Key words: gold nanoparticles, water soluble, 3-aryl-3-(trifluormethyl) diazirine, carbene, photochemistry, surface modification.

Résumé : Des nanoparticules d'or (AuNPs) fonctionnalisée avec de la 3-aryl-3-(trifluorméthyl) diazirine soluble dans un solvant à phases aqueuse et organique ont été préparées par l'intermédiaire d'une réaction d'échange à partir d'AuNP terminées par du monométhyl éther (Me) de triéthylène glycol (EG$_3$). Ces nanoparticules ont été totalement caractérisées à l'aide de la spectroscopie résonance magnétique nucléaire (RMN) ^{1}H et ^{19}F, microscope électronique à transmission (MET), analyse thermogravimétrique (ATG) et spectroscopie d'électrons pour analyse chimique (ESCA). Les données de l'ATG et de la spectroscopie RMN ^{1}H NMR ont permis de déterminer que le taux d'incorporation des ligands de diazirine (Diaz) sur les AuNP monocouches mélangées était de 15% et les images de MET ont mis en évidence un diamètre moyen de 2,3 ± 0,5 nm. Ces renseignements ont permis d'obtenir la formule moléculaire estimée d'Au$_{400}$ (S-EG$_4$-Diaz)$_{40}$ (S-EG$_3$-Me)$_{230}$ pour ces AuNP. Il est à noter que l'ESCA à haute résolution a servi d'outil puissant d'analyse quantitative. L'irradiation des AuNP terminées par de la diazirine entraîne la libération d'azote et la formation d'un carbène hautement réactif, une partie de la réaction passant manifestement par un intermédiaire diazo et nécessitant ainsi un second photon pour l'activation. Les carbènes produits ont été utilisés pour fixer les AuNP en les insérant dans les fonctions C=C ou O–H sur différents substrats. Nous démontrons ici que la photolyse des AuNP modifiés par la diazirine en présence de modèles de capteurs de carbène variés conduit à des produits d'insertion propres et efficaces tout en préservant leur solubilité dans des solvants polaires. [Traduit par la Rédaction]

Mots-clés : nanoparticules d'or, soluble dans l'eau, 3-aryl-3-(trifluorméthyl) diazirine, carbène, photochimie, modification de surface.

Introduction

Gold nanoparticles (AuNPs) possess unique physical and chemical properties that make them outstanding candidates for numerous applications ranging from electronics, catalysis, biology, and sensor science.[1–6] Many of these applications are correlated with the nature of the protecting ligand attached to the gold core. Therefore, developing techniques to prepare nanoparticles with specific moieties or functionalities directly or by means of chemical reactions at the interface of the protecting shells can be a key factor affecting the final AuNP application. Interfacial reactions on the surface of AuNPs can be an outstanding alternative to conventional methods when there is a need to incorporate new functionalities onto the gold surface. A moiety at the gold inter-face that can be thermally or photochemically activated can be utilized as a reactive template for further modification of AuNPs. Such a procedure circumvents the tedious and time consuming chemical synthesis of ligands prior to the AuNP synthesis.

In several cases, compared to other chemical routes, photochemical reactions have the advantage of yielding a product via shorter routes, without the need to carry on several synthetic reactions. Because AuNPs are sensitive to elevated temperatures, they can be subject to loss of the protecting ligands or even decomposition, so another advantage is the possibility of performing photochemical reactions at ambient temperature. Phenyl (trifluoromethyl) diazirine is a popular photoactive group used in photoaffinity labeling for the structural elucidation of biological substrates.[7–9] Diazirine (Diaz) is chemically and thermally stable

S. Ghiassian and M.S. Workentin. Department of Chemistry and the Center for Materials and Biomaterials Research, The University of Western Ontario, London, ON N6A 5B7, Canada.
M.C. Biesinger. Surface Science Western, The University of Western Ontario, 999 Collip Circle, London ON N6G 0J3, Canada.
Corresponding author: Mark S. Workentin (e-mail: mworkent@uwo.ca).

Scheme 1. Cartoon representation of the thiol exchange reaction for the preparation of diazirine/triethylene glycol gold nanoparticles (Diaz-EG$_4$-AuNPs) and their photoinduced carbene generation and reactivity for interfacial modification.
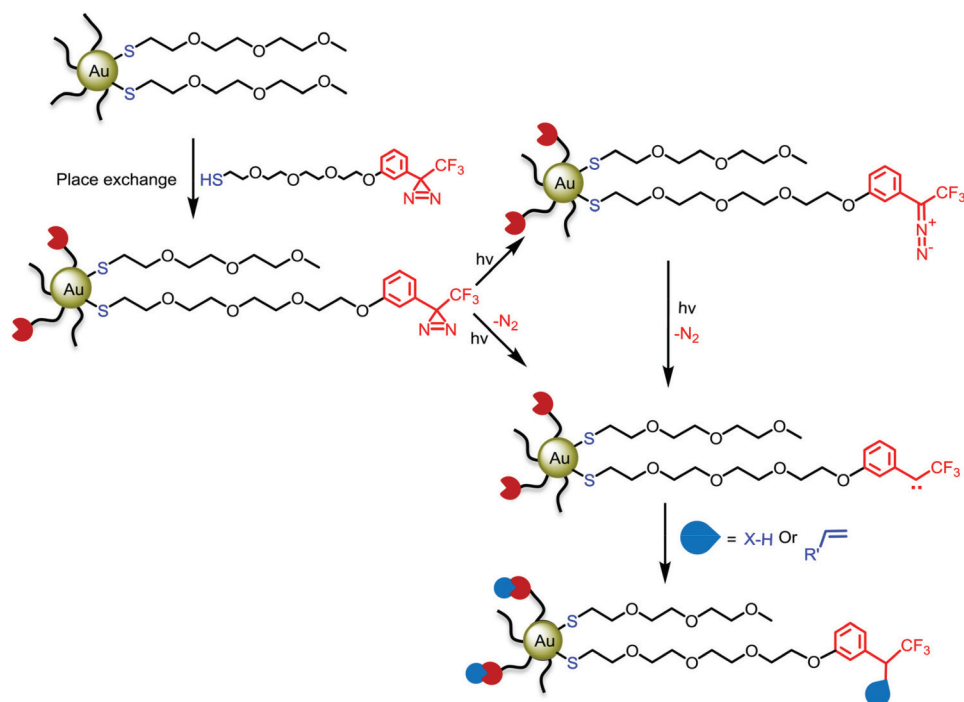
prior to photolysis but can be activated upon irradiation with UV light. When diazirine molecules absorb light at 365 nm, where most biomolecules are transparent, they form a highly reactive carbene intermediate that can initiate an addition reaction with double bonds, insertion into O–H, N–H, S–H, or even C–H functional groups, and form covalent bonds with target substrates that are within molecular vicinity at the time of photoactivation.[7,10] Although mostly used for biological applications, diazirine has remained rather unexplored in other areas such as surface modification of other molecules. Diazirine has been used for the modification of polymeric substrates[10,11] or to incorporate a redox active functional group onto nanomaterials such as carbon nanotubes (CNTs).[12,13] Our group has demonstrated that diazirine functionality can also be a convenient photoprecursor for surface modification when it is attached to a highly fluorinated phosphonium salt. This approach enables preparation of robust hydrophobic surfaces on any material, including cotton and paper, through a simple photochemical treatment.[14]

Recently, we prepared a diazirine/alkanethiolate stabilized gold nanoparticle that is very stable for prolonged periods when kept in the dark, but is able to undergo interfacial reactions upon diazirine photoactivation.[15] These particles proved to be excellent photoprecursors for the introduction of AuNPs to various materials including CNTs, graphene, diamond, and glass.[16–18] Despite all their advantages, the solubility of dodecane diazirine modified AuNPs is limited to a narrow range of organic solvents. The lack of solubility in water or other polar solvents in general limits their application for modification to materials that are soluble or dispersible in nonpolar media.

Ethylene glycol thioalkylated AuNPs have shown great promise for the synthesis of robust water-soluble AuNPs.[19,20] Previously, we developed a straightforward procedure for the synthesis of small water-soluble AuNPs through thiol exchange reactions, using triethylene glycol monomethyl ether functionalized AuNPs as the building blocks. Such AuNPs have the added benefit of solubility in a wide range of organic solvents as well as aqueous media.[21,22] Furthermore, capping the gold core with shorter tri- or

tetra-ethylene glycol chains versus polyethylene glycol thiolates employed previously, allows for producing mixed monolayer protected AuNPs and their complete and straightforward characterization at any stage. Through a combination of characterization techniques such as thermogravimetric analysis (TGA), nuclear magnetic resonance (NMR), and X-ray photoelectron spectroscopy (XPS) one is able to calculate the number of ligands surrounding the gold core. Such information can be further used to determine the ratio of the different ligands after a place exchange reaction has occurred and hence the number of new ligands introduced to the surface.

In this work, we report the synthesis and characterization of a new type of robust, stable, and water-soluble AuNP containing a diazirine moiety at the interface to serve as a photoactivated template to incorporate additional functionality onto the AuNP. Diazirine/triethylene glycol capped AuNPs are prepared through a thiol exchange reaction on small triethylene glycol monomethyl ether particles (Scheme 1). The novel feature of these AuNPs is that it combines the photoreactivity of the diazirine/alkanethiolate-functionalized AuNPs with excellent solubility in water and importantly other polar organic solvents. We believe that such particles can be useful in photochemical immobilization of AuNPs on biomolecules as well as other materials under mild conditions and are not limited for use in a narrow range of solvents.

Experimental

General compounds and instrumentation

The compounds hydrogen tetrachloroaurate(III), sodium borohydride, triethylene glycol monoethyl ether, tetraethylene glycol, 4-dimethylaminopyridine (DMAP), potassium thioacetate, *p*-toluenesulfonyl chloride, 3-bromoanisole, *n*-butyllithium, hydroxylamine hydrochloride, silver nitrate(I), boron tribromide, and ethylvinyl ether were purchased from Sigma-Aldrich and used as received. Deuterated water (D$_2$O), deuterated chloroform (CDCl$_3$), and deuterated methanol (CD$_3$COD) (Cambridge Isotope Laboratories)

were all used as received. All common solvents, triethyl amine, dry methanol, hydrochloric acid, and sodium hydroxide were purchased from Caledon Laboratories Ltd. Glacial acetic acid (99.7%) was purchased from BDH.

^{1}H, ^{13}C, and ^{19}F {^{1}H} NMR spectra were recorded on either a Varian Inova 400 MHz or a Varian Mercury 400 MHz spectrometer. Thermogravimetric analysis (TGA) measurements were recorded by loading the sample in a 70 μL ceramic crucible and heating from 25–750 °C with a rate of 10 °C min^{-1}. The experiments were performed under a nitrogen flow of 70 mL min^{-1} in a Mettler Toledo TGA/SDTA 851 instrument. Transmission electron microscopy (TEM) images were recorded on a TEM Philips CM10. The TEM grids (Formvar carbon film on 400 mesh copper grids) were purchased from Electron Microscopy Sciences and prepared by drop casting a solution of nanoparticles directly onto the grid surface. UV–vis spectra were collected employing a Varian Cary 300 Bio spectrometer. Mass spectrometry measurements were carried out using a Micromass LCT (electrospray time-of-flight) mass spectrometer. The XPS analyses were carried out with a Kratos Axis Ultra spectrometer using a monochromatic Al Kα source (15 mA, 14 kV). The instrument work function was calibrated to give a binding energy (BE) of 83.96 eV for the Au 4f$_{7/2}$ line for metallic gold and the spectrometer dispersion was adjusted to give a BE of 932.62 eV for the Cu 2p$_{3/2}$ line of metallic copper. Specimens were mounted on double sided adhesive tape and the Kratos charge neutralizer system was used on all specimens. Survey scan analyses were carried out with an analysis area of 300 μm × 700 μm and pass energy of 160 eV. High-resolution analyses were carried out with an analysis area of 300 μm × 700 μm and pass energy of 20 eV. Spectra have been charge corrected when needed to the main line of the carbon 1s spectrum set to 285.0 eV for aliphatic carbon. Spectra were analyzed using CasaXPS software (version 2.3.14).

Synthesis

The general synthetic procedure for the preparation of the target thiol, diazirine-EG$_4$-SH, is illustrated in Scheme 2.

Compound 1

All steps in the preparation of **1** were performed in accordance with the literature procedure.[15] Briefly, the reaction of 3-bromoanisole with *n*-butyllithium gave the aryllithium, which was subsequently converted to the corresponding ketone, 2,2,2-trifluoro-1-(3-methoxyphenyl)ethanone, using diethyl trifluoroacetamide. The addition of hydroxylamine hydrochloride to this product yielded an oxime. The oxime was converted to *p*-tolylsulfonyl oxime and then oxidized to give the 3-(3-methoxyphenyl)-3-(trifluoromethyl)-3*H*-diazirine. Later, it was treated with boron tribromide at 0 °C to give the corresponding phenol, 3-(3-hydroxyphenyl)-3-(trifluoromethyl)-3*H*-diazirine (**1**).

^{1}H NMR (400 MHz, CDCl$_3$, ppm) δ: 6.69 (s, 1H), 6.77 (d, 1H), 6.94 (dd, 1H), 7.31 (t, 1H). ^{19}F {^{1}H} (400 MHz, CDCl$_3$, ppm): −65.6.

Compound 2

Compound **2** was synthesized according to the literature procedure[21] by the addition of triethyl amine and 4-dimethylaminopyridine (DMAP) to a solution of tetraethylene glycol.

^{1}H NMR (400 MHz, CDCl$_3$, ppm) δ: 2.45 (singlet, 6H), 3.57 (multiplet, 8H), 3.68 (triplet, 4H, *J* = 8 Hz), 4.16 (triplet, 4H, *J* = 8 Hz), 7.34 (multiplet, 4H), 7.80 (multiplet, 4H).

Compound 3

To 4.1 g (8 mmol) of **2** was added 0.45 g (2.2 mmol) of **1** and they were dissolved in 100 mL of dry acetone. After the solution was purged with argon for 15 min, 370 mg (2.7 mmol) of potassium carbonate was added quickly. The final mixture was purged for 10 more minutes with argon. The reaction solution was stirred under an inert atmosphere for 72 h at room temperature. After reaction completion, acetone was evaporated. Next, the residue was parti-

Scheme 2. Pathway towards the synthesis of Diaz-EG$_4$-SH (**5**).
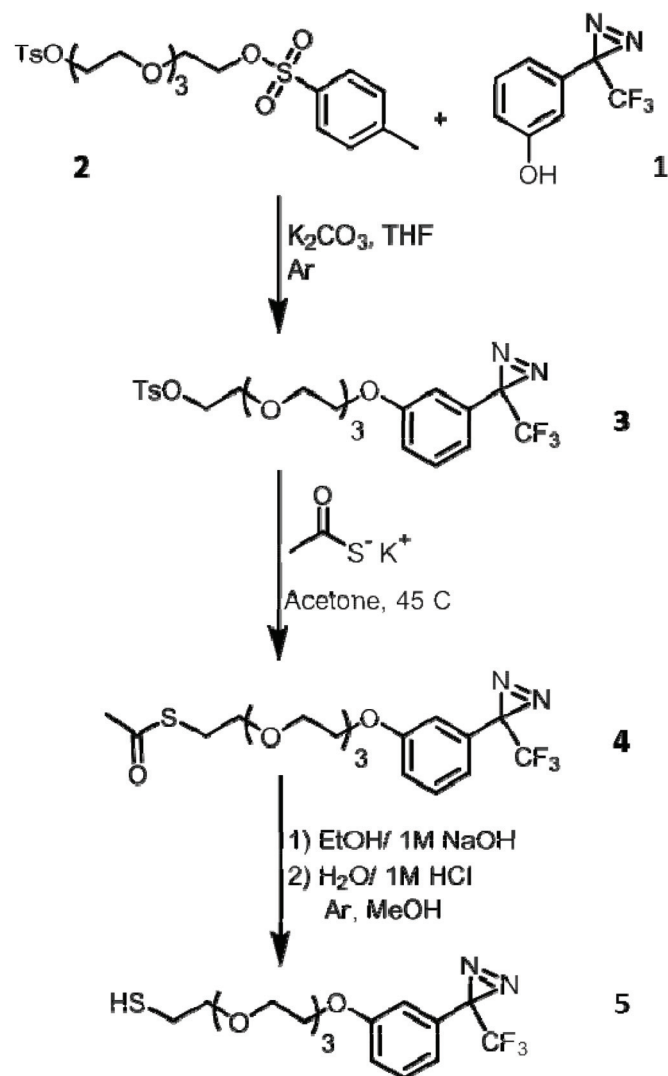
tioned between water (10 mL) and dichloromethane (20 mL). The organic layer was washed with water (3 × 10 mL), dried over MgSO$_4$, filtered, and concentrated. The crude product was used in the next step without further purification.

^{1}H NMR (400 MHz, CDCl$_3$, ppm) δ: 2.4 (s, 3H), 3.6–3.7 (m, 10H), 3.8 (t, 2H), 4.0–4.1 (m, 4H), 6.7 (s, 1H), 6.7 (d, 1H), 6.9 (dd, 1H), 7.2 (t, 1H), 7.3 (d, 2H), 7.8 (d, 2H). ^{19}F {^{1}H} NMR (400 MHz, CDCl$_3$, ppm) δ: −65.2.

Compound 4

To 780 mg (1.46 mmol) of compound **3** was added 217 mg (1.9 mmol) of potassium thioacetate and then they were dissolved in 25 mL of acetone and refluxed at 50 °C overnight. After reaction completion, the mixture was filtered and the solvent was evaporated. The residue was partitioned between water (10 mL) and dichloromethane (20 mL). The organic layer was washed three times with brine and dried over MgSO$_4$. After filtration, the solvent was evaporated to afford **4**. Purification of the crude product by column chromatography (1:1 ethylacetate/hexanes) gave **4** in a quantitative yield as a yellow oil.

^{1}H NMR (400 MHz, CDCl$_3$, ppm) δ: 2.3 (s, 3H), 3.1 (t, 2H), 3.6–3.7 (m, 10H), 3.9 (t, 2H), 4.1 (t, 2H), 6.7 (s, 1H), 6.8 (d, 1H), 6.9 (dd, 1H), 7.3 (t, 1H). ^{13}C NMR (400 MHz, CDCl$_3$, ppm) δ: 28.8, 30.5, 41.7, 67.5, 69.5, 69.7, 70.3, 70.5, 70.6, 70.8, 113.0, 115.7, 118.8, 129.9, 130.4, 158.9, 195.4. ^{19}F {^{1}H} NMR (400 MHz, CDCl$_3$, ppm) δ: −65.2. MS *m/z* calculated for C$_{18}$H$_{23}$F$_3$N$_2$O$_5$S: 436.128; found: 436.127.

Compound 5

Dry methanol (2 mL) was used to dissolve 60 mg (0.2 mmol) of compound **4** and the solution was purged with argon for 15 min. In a separate flask, 120 μL of 1 mol/L NaOH solution in EtOH was purged with argon for 15 min. Using a cannula, the base solution was transferred to the methanol solution and the reaction mixture was stirred under an inert atmosphere for 45 min. In the meantime, 250 μL of 1 mol/L HCl in Milli-Q water was purged with argon in a third flask for 15 min. After the 45 min period, the acid solution was transferred to the reaction mixture using a cannula. The solution was then stirred for 10 min under argon. Next, the reaction was stopped and the thiol was extracted with dichloromethane. After three consecutive extractions, all the combined organic phases were dried over MgSO$_4$. After filtration, the solvent was removed under reduced pressure to afford compound **5** as a yellow oil in a quantitative yield.

^{1}H NMR (400 MHz, CDCl$_3$, ppm) δ: 1.6 (t, 1H), 2.7 (q, 2H), 3.6–3.7 (m, 10H), 3.9 (t, 2H), 4.1 (t, 2H), 6.7 (s, 1H), 6.8 (d, 1H), 6.9 (dd, 1H), 7.3 (t, 1H). ^{13}C NMR (400 MHz, CDCl$_3$, ppm) δ: 28.2, 29.0, 67.4, 69.3, 69.4, 69.9, 70.1, 70.3, 112.7, 115.7, 118.4, 129.9, 130.1, 159.3, 195.6. ^{19}F {^{1}H} NMR (400 MHz, CDCl$_3$, ppm) δ: −65.2. MS m/z calculated for C$_{16}$H$_{21}$F$_3$N$_2$O$_4$S: 394.117; found: 394.116.

Preparation of diazirine modified AuNPs (Diaz-EG$_4$-AuNPs)

Diazirine modified AuNPs were synthesized through a place exchange reaction. First, triethylene glycol monomethyl ether AuNPs (Me-EG$_3$-AuNPs) were synthesized in accordance with our previously reported procedure.[21] Next, to introduce the diazirine tetraethylene glycol thiol ligands onto the nanoparticle shell, 5 mg of freshly prepared thiol **5** was dissolved in 1 mL of MeOH/acetone (8:2). This solution was then added to a solution of Me-EG$_3$-AuNPs (25 mg in 10 mL of MeOH/acetone (8:2)). After vigorously stirring the reaction mixture for 10 min, the solvent was evaporated to form a film of nanoparticles. This film was washed with cyclohexane (×3) to remove the excess diazirine thiol **5**.

^{1}H NMR (400 MHz, D$_2$O, ppm) δ: 3.1–3.4 (broad), 3.5–4.2 (broad), 6.5–6.6 (broad), 6.8–7.0 (broad), 7.1–7.3 (broad). ^{19}F {^{1}H} NMR (400 MHz, D$_2$O, ppm) δ: −65.7.

Photochemical modification of Diaz-EG$_4$-AuNPs

Diaz-EG$_4$-AuNP (10 mg) was dissolved in 10 mL of benzene and 10 equiv. of the target substrate (methanol, ethylvinyl ether, or acetic acid) was added. The mixture was transferred to a Pyrex flask (filters light below 300 nm) and purged with argon for 15 min. The sample was then irradiated using a medium pressure mercury lamp (Hanovia S9 PC 451050/805221), which was contained in a quartz water jacket, approximately 10 cm from the flask. After reaction completion (the time for disappearance of diazirine, followed by ^{19}F NMR spectroscopy), all of the solvent was evaporated to form a film of nanoparticles. The film was then washed with cyclohexane (×3) to remove any unreacted substrate from the modified AuNPs. Over the course of the reaction, in the ^{19}F NMR spectra, the signal at −65 ppm, which is representative of the CF$_3$ group of the diazirine, gradually disappeared and a new signal appeared corresponding to the product formed via the carbene insertion.

Results and discussion

To prepare the 3-aryl-3-(trifluoromethyl) diazirine modified AuNPs (Diaz-EG$_4$-AuNPs), we utilized a place exchange reaction incorporating 3-aryl-3-(trifluoromethyl) diazirine tetraethylene glycol thiolate (Diaz-EG$_4$-SH) onto small triethylene glycol monomethyl ether modified AuNPs as illustrated in Scheme 1.

3-(3-Hydroxyphenyl)-3-(trifluoromethyl)-3*H*-diazirine (**1**) was synthesized according to previous reports[15] and was then used in the preparation of Diaz-EG$_4$-SH (**5**) according to Scheme 2.

Me-EG$_3$-AuNPs were prepared according to our previously reported literature procedure.[21] It is important to note that methyl

Fig. 1. (A) ^{1}H NMR spectrum of the Me-EG$_3$-AuNPs. (B) and (C) ^{1}H and ^{19}F NMR spectra, respectively, of the Diaz-EG$_4$-AuNP (recorded in D$_2$O). (D) and (E) ^{1}H and ^{19}F NMR spectra, respectively, of the Diaz-EG$_4$-SH (recorded in CDCl$_3$).
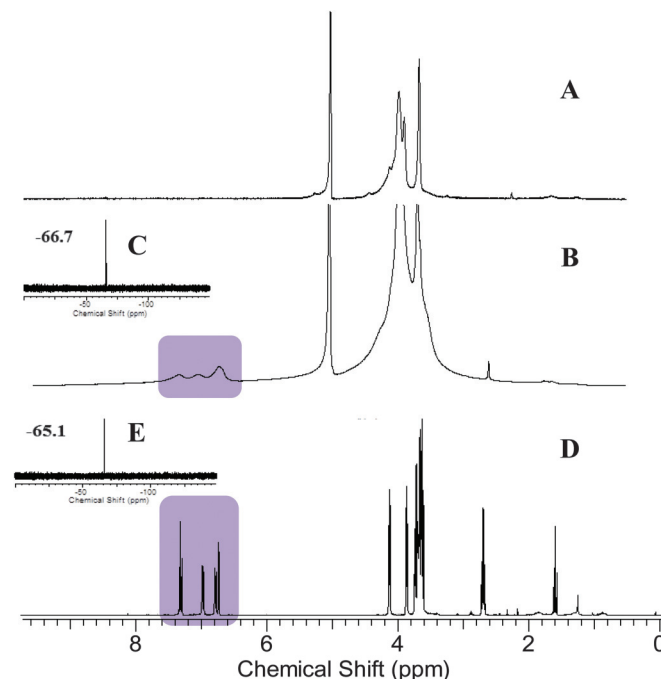
terminated triethylene glycol stabilized AuNPs were selected as the basic building block for the synthesis of water-soluble AuNPs for several reasons: While oxygenated chains of the triethylene glycol ligand allows water solubility of the particles, unlike the more commonly used citrate capped gold clusters that are charged and prone to agglomeration on removal of the solvent, thiolate triethylene glycol stabilized particles remain stable after solvent evaporation and can be redissolved in the solvent. Additionally, incorporating triethylene glycol monomethyl ether ligands onto the gold core enables solubility in a range of organic solvents as well as water. Consequently, such nanoparticles can be used in a wide range of organic (both polar and nonpolar) or aqueous media for various applications. Also, unlike polyethylene glycol (PEG) stabilized AuNPs, these short chain triethylene glycol building blocks allow the use of thiol exchange reactions to incorporate new functionalities on the gold core in one easy step. They can then be fully characterized through several complementary techniques such as NMR, TGA, TEM, and XPS.

After the synthesis of Me-EG$_3$-AuNPs, they were subsequently subjected to a place exchange reaction in the presence of Diaz-EG$_4$-SH (**5**) in a mixture of acetone and methanol. In a typical exchange reaction, Me-EG$_3$-AuNPs (100 mg) and Diaz-EG$_4$-SH (20 mg) were stirred in a mixture of MeOH/acetone (8:2). After 10 min, the solvent was removed under reduced pressure to stop the exchange reaction and form a film. The film was then washed with cyclohexane to remove any unreacted thiol **5** or any disulfide that might have formed during the synthetic procedure. Initially, the success of the place exchange reaction was confirmed by means of ^{19}F and ^{1}H NMR spectroscopy (see Fig. 1). The ^{1}H NMR spectrum of the Diaz-EG$_4$-AuNPs (recorded in D$_2$O) exhibits the expected broad peaks at δ$_H$ 3–4.2 ppm due to the methyl and methylene groups present in the triethylene glycol chains. In addition, after the place exchange reaction, three broad peaks appear in the aromatic region (δ$_H$: 6.5, 6.9, and 7.2 ppm). These new signals can be assigned to the aromatic protons of the 3-aryl-3-(trifluoromethyl) diazirine moiety, when the ^{1}H NMR spectrum of the Diaz-EG$_4$-AuNPs is compared to

Fig. 2. TGA graphs of Me-EG$_3$-AuNP (dashed lines) and Diaz-EG$_4$-AuNP (solid lines): Mass loss curves (left) and the first derivative of the mass loss curves (right).
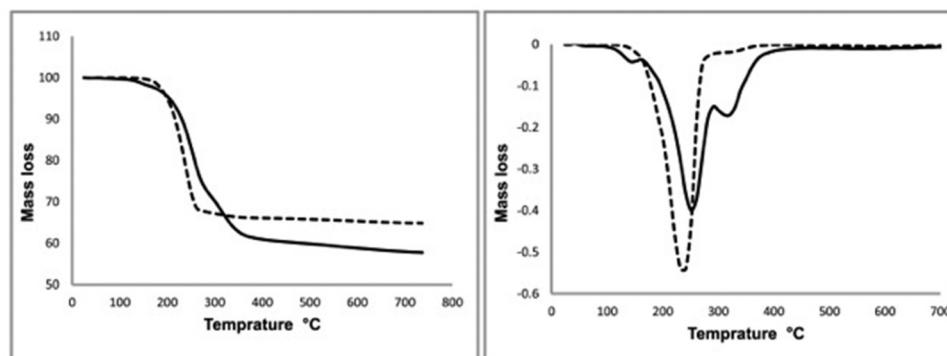
the corresponding spectrum of the free diazirine thiol **5** (Figs. 1B and 1D). In addition, the signals at 1.6 and 2.7 ppm present in the free thiol spectrum, which are respectively due to the thiol proton (SH) and methylene group α to the sulfur (CH$_2$-SH), disappear after the place exchange reaction, which further confirms binding of the sulfur to the gold. Also important is the lack of any sharp signals in the ^{1}H NMR spectrum of the final AuNPs. This confirms the effectiveness of the washing protocol in removing any unbound thiol **5** or disulfide. Through the integration of either of the three signals in the aromatic region relative to the integration of the peak at 3.3 ppm that corresponds to the three protons of the methyl group of the Me-EG$_3$-S-ligands, it was possible to determine that 15% of the protecting ligands are comprised of Diaz-EG$_4$-S-, while 85% consist of Me-EG$_3$-S-. It is noteworthy that while these AuNPs are soluble in organic media, our goal is to balance the extent of diazirine ligand incorporation while maintaining water solubility. The composition 85:15 allows the amphiphilic property of the AuNP to be retained and therefore permit the subsequent photochemical modification in either organic or aqueous media. A longer exchange reaction time leads to a higher incorporation of Diaz-EG$_4$-SH ligands onto the gold core (>20%), but results in a significant decrease in the water solubility of the final particles. Also, the choice of solvent for the place exchange reaction has a major effect on the solubility of the final AuNPs. Because the thiol exchange reaction (to the extent that it does not harm the water solubility) happens in a matter of minutes, we used an acetone/methanol mixture, which allows faster and more efficient removal of the free thiols after the place exchange.

Due to the presence of the CF$_3$ group, further characterization of the particles can be achieved using ^{19}F NMR spectroscopy. The fluorine atoms of the CF$_3$ group give rise to a signal at −66.7 ppm when the NMR spectrum is measured in D$_2$O or −65.2 ppm when measured in CDCl$_3$, which confirms the incorporation of the diazirine functionality onto the gold core (Fig. 1C). Additionally, the fluorine signal can be later employed to follow the photomodification reactions of Diaz-EG$_4$-AuNPs. It is important to note that the NMR spectra of Diaz-EG$_4$-AuNPs were collected in D$_2$O to demonstrate their excellent water solubility. However, the corresponding Diaz-EG$_4$-SH is characterized in CDCl$_3$ mainly because of their lower solubility in water. The slight difference in the chemical shifts of the fluorine signals, −65.1 vs −66.7 ppm in the free thiol and Diaz-EG$_4$-AuNPs, respectively, is only due to the solvent effects.

From TGA data, we can obtain information about the quantity of the organic ligands attached to the gold core. Both Me-EG$_3$-AuNPs and Diaz-EG$_4$-AuNPs were examined using TGA (Fig. 2). Comparison of the two TGA profiles confirms the presence of the diazirine moiety. The total mass loss for Me-EG$_3$-AuNP is 35.7% when heated from 25–750 °C. However, in the case of Diaz-EG$_4$-AuNP, the total mass loss is 42.3% and the first mass loss observed

at ~100 °C is 6.6% of the total mass loss (calculated from the ratio of the peak areas in the first derivative of the TGA curve; Fig. 2, left graph). Assuming all this mass loss at ~100 °C is due to the nitrogen extrusion from the diazirine ring, the ratio of the diazirine ligands to the triethylene glycol ligands will be 15:85, which is consistent with the ^{1}H NMR analysis. Using the TGA and TEM data, and assuming that the gold core has a spherical shape, we can determine a simplified formula of Au$_{400}$ (S-EG$_4$-Diaz)$_{40}$ (S-EG$_3$-Me)$_{230}$ for the Diaz-EG$_4$-AuNPs.

XPS analysis further confirmed the successful preparation of Diaz-EG$_4$-AuNPs and the ratio between the two different ligands on the gold core. The Au $4f_{7/2}$ core line appears at 84.3 eV that is shifted to a binding energy higher than that of the bulk gold (83.95 eV) due to particle size effects.[23] The S 2p core line shows the presence of two major components, the S 2p$_{3/2}$ at 162.8 eV and S 2p$_{1/2}$ at 164.0 eV, in a 2:1 spin orbit splitting ratio for the Au–S bonds.[24] (See the Supplementary data.) Finally, the high-resolution scan of the C 1s peak, F 1s peak, and N 1s peak (see Fig. 3) confirmed the presence of the diazirine functional group on the gold core. The C 1s core line shows the appearance of a component at 292.8 eV typical of the CF$_3$ group. The F 1s core line also shows the emergence of a peak at 688.4 eV. From the molecular structure of the two ligands that surround the gold core and from the relative percentages of the C 1s component at 292.8 eV and that at 286.3 eV related to the C–O of the ethylene glycol units of both the ligands, the composition of the organic layer protecting the gold core can be estimated with good precision. Through this independent method, we could confirm that 15% ± 2% of the ligands are Diaz-EG$_4$-S-, which was also estimated from the integration of the ^{1}H NMR spectrum (vide supra). See the Supplementary data for details on the calculation.

Photochemical modification of Diaz-EG$_4$-AuNPs through carbene insertion reactions

The UV–vis spectrum of the Diaz-EG$_4$-SH exhibits an absorption band around 350 nm due to the presence of the diazirine ring (see the Supplementary data). Upon irradiation of Diaz-EG$_4$-AuNPs with a medium pressure Hg lamp (λ > 300 nm), the diazirine loses N$_2$ and generates a highly reactive carbene that can then undergo insertion (into X–H bonds) or addition (to alkenes) reactions. At least a certain percentage of the irradiated diazirine forms the diazo compound (as can be observed in Fig. 4). However, further irradiation of the diazo isomer will lead to the generation of the carbene as well. The course of photochemical reactions can be monitored using ^{19}F NMR spectroscopy through the disappearance of the signal at −65 ppm (corresponding to the CF$_3$ of the diazirine) and the appearance of new signals in the ^{19}F NMR spectrum.

To demonstrate that we can further modify the nanoparticles using the diazirine functionality as a template, we studied the photolysis of Diaz-EG$_4$-AuNPs in the presence of different carbene

Fig. 3. High-resolution XPS spectra of Me-EG$_3$-AuNP and Diaz-EG$_4$-AuNP.
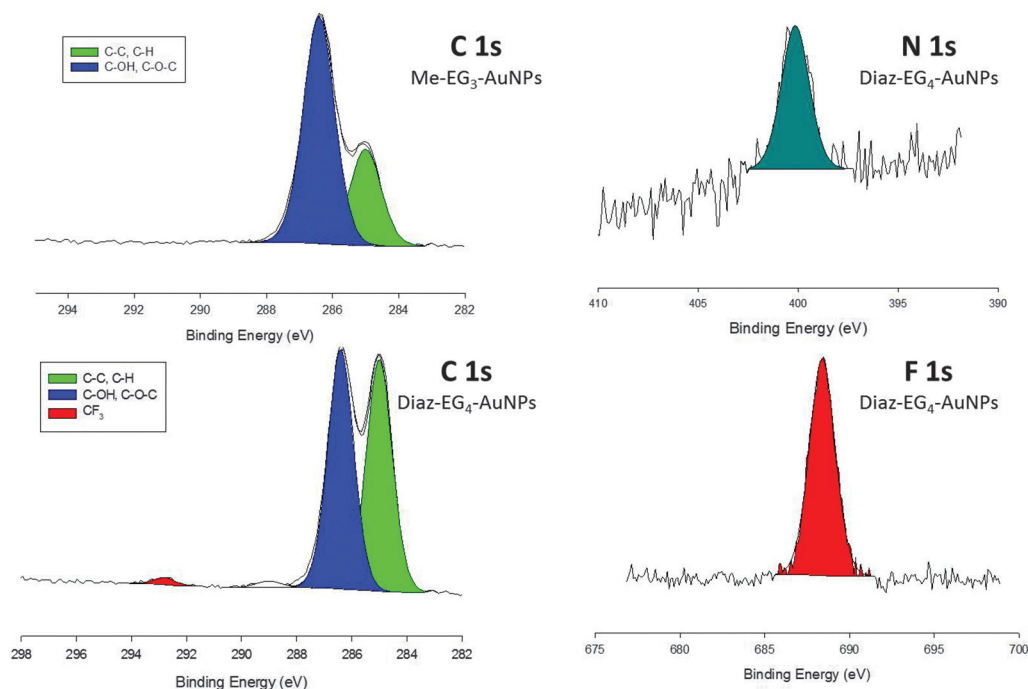
Fig. 4. ^{19}F NMR spectrum of Diaz-EG$_4$-AuNPs in methanol during photolysis at different times: (A) $t = 0$, (B) $t = 90$ min, and (C) $t = 12$ h.
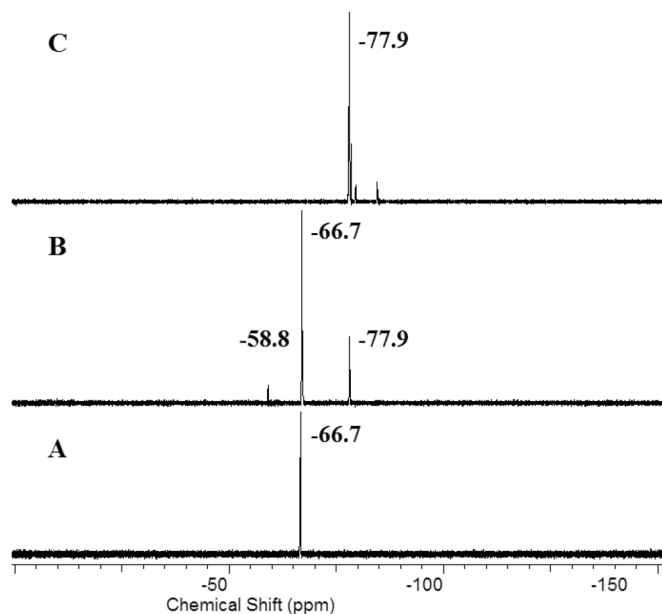

trapping agents. As a simple proof of concept, we chose methanol as our first carbene scavenger. A solution of Diaz-EG$_4$-AuNPs and methanol in benzene was purged with argon for 15 min and sealed to avoid any oxygen. The mixture was then irradiated at λ > 300 nm and the progress of the reaction was monitored using ^{19}F NMR spectroscopy. Through the photochemical reaction of methanol with the diazirine modified AuNPs (Fig. 4), the ^{19}F NMR spectrum exhibits three distinct signals: (*i*) The signal at −66.7 ppm that is due to the parent diazirine and decreases in intensity over time. (*ii*) The signal at −58 ppm that can be attributed to the diazo intermediate formed upon photolysis (see Scheme 1).[11,15] This peak initially grows and then disappears upon continued irradia-

tion. (*iii*) The signal at −77.9 ppm that emerges due to the insertion of the carbene into the O–H bond and increases in intensity as the reaction moves towards completion.[11,15] No C–H insertion product was observed, as the ^{19}F NMR spectrum showed only a single signal after reaction completion.

To prove that we can obtain a clean insertion reaction product if O–H bonds are available, we repeated the same photochemical protocol for acetic acid as another model reaction. Ethyl vinyl ether was also used as a model to examine the reactivity of the photogenerated carbene towards alkenes. All the products were characterized using ^{1}H and ^{19}F NMR spectroscopy, which showed a complete conversion of Diaz-EG$_4$-AuNPs to the corresponding insertion products. ^{19}F NMR spectra showed complete conversion to the desired products as the signal at −66.7 ppm disappeared and new signals appeared depending on the substrate used (Fig. 5). In the case of insertion into methanol, where the product has a ^{19}F NMR signal at −77.9 ppm, insertion into the alkene of ethyl vinyl ether gives two signals at −63.5 and −69.4 ppm due to the two diastereomers formed on insertion to form the cyclopropane, and insertion into the O–H of acetic acid exhibits a signal at −77.5 ppm.[11,15] The formation of the products was also confirmed by the appearance of new peaks in ^{1}H NMR spectra (see the Supplementary data). While photochemical modification proceeds efficiently, due to the increase in the organic character of the target molecules, solubility of the AuNPs changed after the photochemical reactions. Water solubility of the particles decreased, while they remain perfectly soluble in other polar solvents such as methanol or acetonitrile. To address this solubility issue and to obtain clear signals in the NMR spectra with a high signal to noise ratio, we conducted all the NMR measurements in deuterated methanol.

It has been previously reported that the photogenerated carbene from aryl-3-(trifluoromethyl)-diazirine is highly reactive towards O–H bonds.[14,15] Carbohydrates are one of the most common biomolecules in living cells with available O–H bonds for insertion of the carbene. Carbohydrate-functionalized gold nanoparticles have gained great attention as drug delivery vehicles and cellular probes. Such materials have been used as biolabels for the study of carbohydrate–carbohydrate or carbohydrate–protein interactions.[25,26] To explore the ability of the reactive carbene to

Fig. 5. Cartoon representation of (A) Diaz-EG$_4$-AuNP and its carbene insertion products (left) and their ^{19}F NMR spectra (right) with (B) methanol, (C) ethyl vinyl ether, and (D) acetic acid.
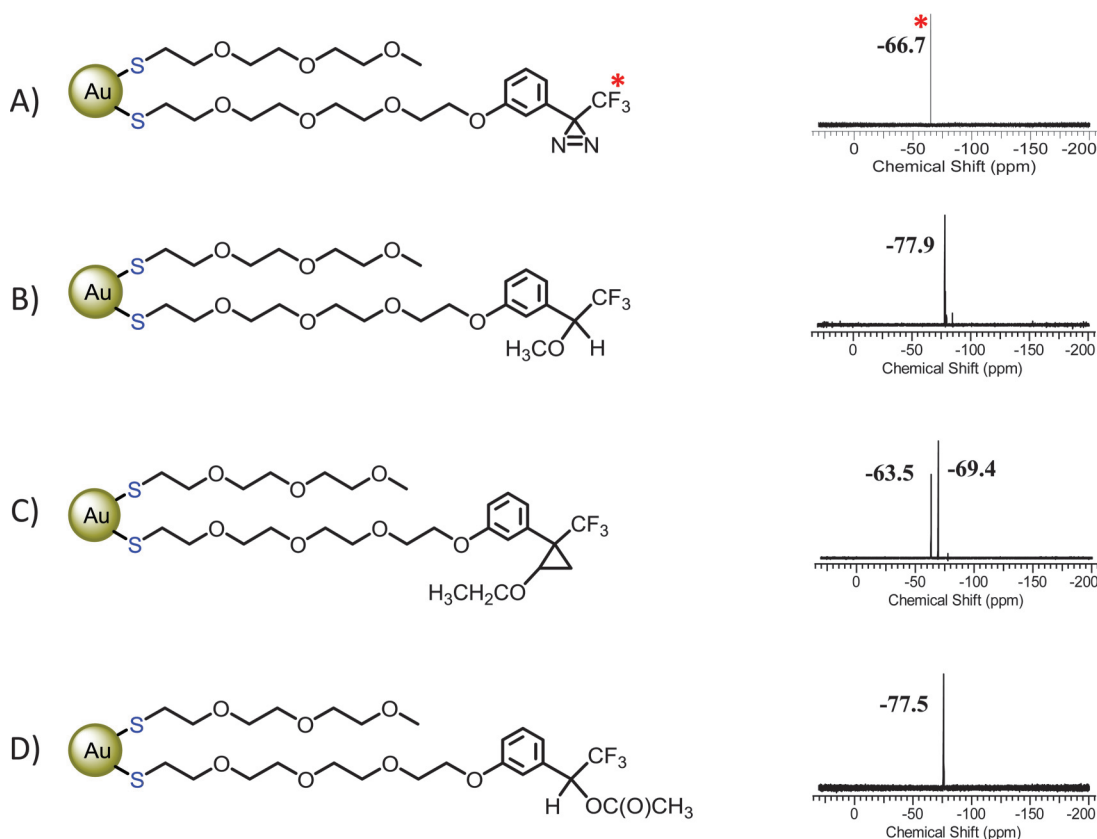

Fig. 6. Cartoon representation of photolysis of Diaz-EG$_4$-AuNP in the presence of mannose and the formation of the desired insertion product (right) and ^{19}F NMR spectra of the reaction products in different concentrations (left).
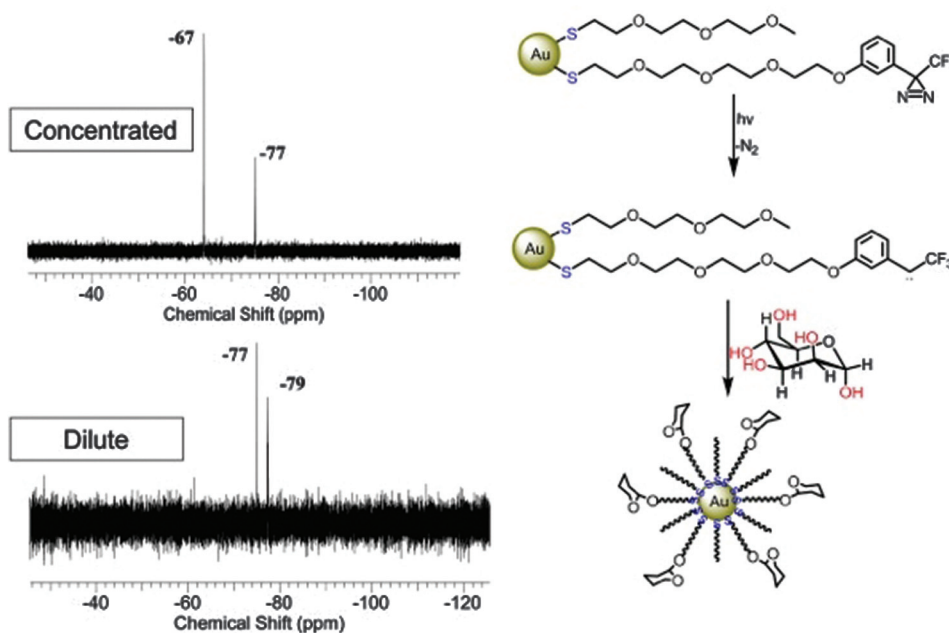
serve as a template to modify the AuNPs in aqueous solutions, we used nonderivatized mannose as a proof of principle. Mannose is a carbohydrate with numerous accessible hydroxyl groups for the reaction with carbene. In a typical experiment, a solution of Diaz-EG$_4$-AuNPs and excess mannose in Milli-Q water was purged with

argon for 15 min and then irradiated in a Pyrex vessel ($\lambda > 300$ nm). The progress of photolysis was followed using ^{19}F NMR. When a concentrated solution of AuNPs (10 mg of AuNPs in 1 mL of Milli-Q water) was used for photolysis, ^{19}F NMR spectrum showed the formation of the azine as the major product (δ_F: −67 ppm) resulting

Fig. 7. TEM images of (A) Me-EG$_3$-AuNP, (B) Diaz-EG$_4$-AuNP, and the insertion products of Diaz-EG$_4$-AuNP with (C) methanol, (D) acetic acid, and (E) ethyl vinyl ether.
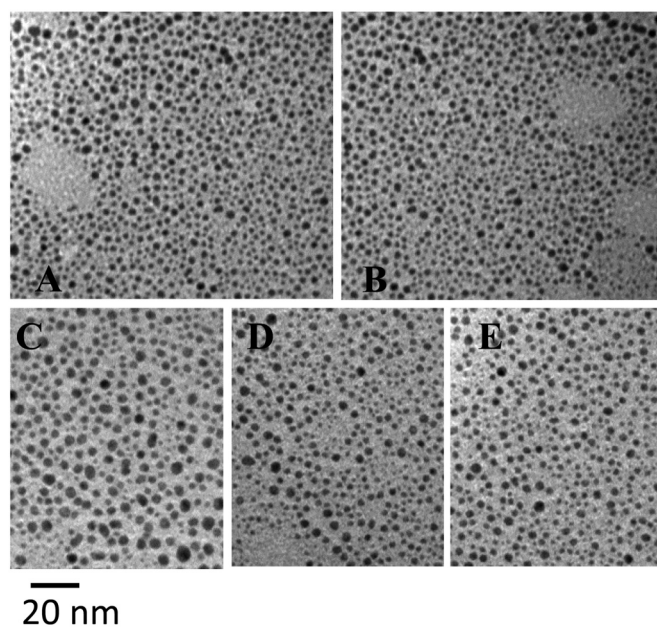
from the reaction of a carbene with a diazo intermediate and the minor product of insertion into O–H bonds of mannose (δ_F: –77 ppm). When a more dilute solution (10 mg of AuNPs in 10 mL of Milli-Q water) was prepared to prevent any dimerization, a signal at –77 ppm appeared as the major component, which can be attributed to the desired product of the insertion into the hydroxyl groups of the mannose. However, water insertion also occurred to some extent, which can be verified by the signal at δ_F –79 ppm (Fig. 6).[11] Although these results demonstrate that we can construct mannose capped AuNPs through photochemical reaction of diazirine, the efficiency of such reactions are lower due to the lower reactivity of the mannose OH and the unspecific reactivity of the carbene towards each other or solvent molecules in their vicinity.

To study the effect of UV irradiation on the size of the particles we used TEM (Fig. 7). The average size of the Diaz-TEG-AuNPs was measured to be 2.3 ± 0.5 nm before photomodification. As Fig. 7 shows, there is no distinct change in the size or shape of the gold core after photolysis and the average size is 2.3 ± 0.7 nm after surface modification. This confirms that UV irradiation has no effect on the size of the particles.

Conclusions

In this work, we have described the synthesis and characterization of small water- and organic-soluble diazirine-functionalized AuNPs. The Diaz-EG$_4$-AuNPs were characterized through ^{1}H and ^{19}FNMR spectroscopy, TGA, TEM, and high-resolution XPS and the amount of diazirine functionality on the corona was estimated with good precision through two independent methods (15% of the total ligands). In particular, we demonstrated that XPS is a powerful tool for quantifying the newly introduced moieties after a place exchange reaction with rather high precision. The unique feature of Diaz-EG$_4$-AuNPs is their amphiphilic character, which expands their potential applications. Due to the presence of the

diazirine moiety, these AuNPs generate a highly reactive carbene upon photolysis. We have demonstrated here that the diazirine functionality can act as an effective template that can be used for further modification of AuNPs through insertion reactions with O–H and C=C bonds, while maintaining their solubility in polar solvents.

Supplementary data

Supplementary data (NMR spectra of compounds **3**, **4**, **5**, Me-EG$_3$-AuNP, Diaz-EG$_4$-AuNP, and all the corresponding photochemically modified products, UV–vis spectra of Me-EG$_3$-AuNP, Diaz-EG$_4$-AuNP, and the insertion products, TGA and high-resolution XPS data, and photograph of Diaz-EG$_4$-AuNPs when it is in water) are available with the article through the journal Web site at http://nrcresearchpress.com/doi/suppl/10.1139/cjc-2014-0287.

References

(1) Jain, P. K. Angew. Chem. Int. Ed. **2014**, 53, 1197. doi:10.1002/anie.201309807.
(2) Hutchings, G. J.; Brust, M.; Schmidbaur, H. Chem. Soc. Rev. **2008**, 37, 1759. doi:10.1039/b810747p.
(3) Corma, A.; Hermenegildo, G. Chem. Soc. Rev. **2008**, 37, 2096. doi:10.1039/B707314N.
(4) Tiwari, P. M.; Vig, K.; Dennis, V. A.; Singh, S. R. Nanomaterials **2011**, 1, 31. doi:10.3390/nano1010031.
(5) Daniel, M. C.; Astruc, D. Chem. Rev. **2004**, 104, 293. doi:10.1021/cr030698.
(6) Saha, K.; Agasti, S. S.; Kim, C.; Li, X.; Rotello, V. M. Chem. Rev. **2012**, 112, 2739. doi:10.1021/cr2001178.
(7) Hashimoto, M.; Hatanaka, Y. Eur. J. Org. Chem. **2008**, 2008, 2513. doi:10.1002/ejoc.200701069.
(8) Blencowe, A.; Hayes, W. Soft Matter **2005**, 1, 178. doi:10.1039/b501989c.
(9) Dubinsky, L.; Kromb, B. P.; Meijler, M. M. Bioorg. Med. Chem. **2012**, 20, 554. doi:10.1016/j.bmc.2011.06.066.
(10) Blencowe, A.; Costick, K.; Hayes, W. New J. Chem. **2006**, 30, 53. doi:10.1039/b514205a.
(11) Blencowe, A.; Caiulo, N.; Cosstick, K.; Fagour, W.; Heath, P.; Hayes, W. Macromolecules **2007**, 40, 939. doi:10.1021/ma061951l.
(12) Lawrence, E. J.; Wildgoose, G. G.; Aldous, L.; Wu, Y. A.; Warner, J. H.; Compton, R. G.; McNaughter, P. D. Chem. Mater. **2011**, 23, 3740. doi:10.1021/cm201461w.
(13) Wildgoose, G. G.; Lawrence, E. J.; Bear, J. C.; McNaughter, P. D. Electrochem. Commun. **2011**, 13, 1139. doi:10.1016/j.elecom.2011.07.015.
(14) Ghiassian, S.; Ismaili, H.; Lubbock, B. D.; Dube, J. W.; Ragogna, P. J.; Workentin, M. S. Langmuir **2012**, 28, 12326. doi:10.1021/la301975u.
(15) Ismaili, H.; Lee, S.; Workentin, M. S. Langmuir **2010**, 26, 14958. doi:10.1021/la102621h.
(16) Ismaili, H.; Lagugne-Labarthet, F.; Workentin, M. S. Chem. Mater. **2011**, 23, 1519. doi:10.1021/cm103284g.
(17) Ismaili, H.; Workentin, M. S. Chem. Commun. **2011**, 47, 7788. doi:10.1039/c1cc12125a.
(18) Ismaili, H.; Geng, D.; Kantzas, T. T.; Sun, X.; Workentin, M. S. Langmuir **2011**, 27, 13261. doi:10.1021/la202815g.
(19) Wuelfing, W. P.; Gross, S. M.; Miles, D. T.; Murray, R. W. J. Am. Chem. Soc. **1998**, 120, 12696. doi:10.1021/ja983183m.
(20) Kannars, A. G.; Kamounah, F. S.; Schaumburg, K.; Kiely, C. J.; Brust, M. Chem. Commun. **2002**, 2294. doi:10.1039/B207838B.
(21) Gobbo, P.; Workentin, M. S. Langmuir **2012**, 28, 12357. doi:10.1021/la302168g.
(22) Gobbo, P.; Novoa, S.; Biesinger, M.; Workentin, M. S. Chem. Commun. **2013**, 49, 3982. doi:10.1039/c3cc41634h.
(23) Bourg, M. C.; Badia, A.; Lennox, R. B. J. Phys. Chem. B **2000**, 104, 6562. doi:10.1021/jp9935337.
(24) Castner, D. G.; Hinds, K.; Grainger, D. W. Langmuir **1996**, 12, 5083. doi:10.1021/la960465w.
(25) Rojo, J.; Diaz, V.; De la Fuente, J. M.; Segura, I.; Barrientos, A. G.; Riese, H. H.; Bernad, A.; Penades, S. ChemBioChem **2004**, 5, 291. doi:10.1002/cbic.200300726.
(26) Reichardt, N. C.; Lomas, M. M.; Penades, S. Chem. Soc. Rev. **2013**, 42, 4358. doi:10.1039/c2cs35427f.